

**Lomonosov Moscow State University**

---

**Skobeltsyn Institute of Nuclear Physics**

**B.S.Ishkhanov, V.N.Orlin, N.N.Peskov, M.E.Stepanov,  
V.V.Varlamov**

**SYSTEMATIC DISAGREEMENTS BETWEEN PARTIAL  
PHOTONEUTRON REACTIONS CROSS SECTIONS:  
NEW APPROACH TO ANALYSIS AND EVALUATION**

MSU SINP Preprint 2013–1/884

**B.S.Ishkhanov, V.N.Orlin, N.N.Peskov, M.E.Stepanov,  
V.V.Varlamov  
e-mail: Varlamov@depni.sinp.msu.ru**

**SYSTEMATIC DISAGREEMENTS BETWEEN PARTIAL PHOTONEUTRON  
REACTIONS CROSS SECTIONS:  
NEW APPROACH TO ANALYSIS AND EVALUATION**

MSU SINP Preprint 2013–1/884

Abstract

There are well-known systematic disagreements in partial photoneutron reaction cross sections data obtained in experiments with quasimonoenergetic annihilation photons using methods of neutron multiplicity sorting. Using proposed criteria we found that major sources of data large systematic uncertainties come from certain shortcomings of experimental methods for outgoing neutron multiplicity sorting. To develop methods of correcting the data obtained in various experiments a new approach for their evaluation was developed in which the equations of a combined model of photonuclear reactions are used to decompose the experimental total neutron yield reaction cross section into contributions of partial reactions. Evaluated cross sections of partial photoneutron reactions obtained by using such method are in agreement with experimental data obtained by alternative experiments. Evaluated partial photoneutron reactions cross sections for  $^{91,94}\text{Zr}$ ,  $^{115}\text{In}$ ,  $^{159}\text{Tb}$ ,  $^{181}\text{Ta}$ ,  $^{188,189,190,192}\text{Os}$ , and  $^{208}\text{Pb}$  are presented.

**Б.С.Ишханов, В.Н.Орлин, Н.Н.Песков, М.Е.Степанов, В.В.Варламов**

**СИСТЕМАТИЧЕСКИЕ РАСХОЖДЕНИЯ СЕЧЕНИЙ ПАРЦИАЛЬНЫХ  
ФОТОНЕЙТРОННЫХ РЕАКЦИЙ:  
НОВЫЙ ПОДХОД К АНАЛИЗУ И ОЦЕНКЕ**

Препринт НИИЯФ МГУ 2013–1/884

Аннотация

Хорошо известны систематические расхождения данных о сечениях парциальных фотонейтронных данных, полученных в экспериментах с квазимоноэнергетическими аннигиляционными фотонами с помощью методов разделения фотонейтронов по множественности. С использованием разработанных критериев было установлено, что основным источником значительных систематических погрешностей данных являются определенные недостатки экспериментальных методов разделения образующихся нейтронов по множественности. Для разработки методов корректировки данных, полученных в различных экспериментах, разработан новый подход для их оценки, заключающийся в том, что для разделения экспериментального сечения реакции полного выхода нейтронов на вклады от сечений парциальных реакций используются уравнения комбинированной модели фотоядерных реакций. Оцененные таким методом сечения парциальных реакций согласуются с результатами альтернативных экспериментов. Представлены оцененные сечения парциальных фотонейтронных реакций для ядер  $^{91,94}\text{Zr}$ ,  $^{115}\text{In}$ ,  $^{159}\text{Tb}$ ,  $^{181}\text{Ta}$ ,  $^{188,189,190,192}\text{Os}$ ,  $^{208}\text{Pb}$ .

## Introduction

The information on cross sections of partial photoneutron reactions with different number of outgoing particles, primarily  $(\gamma, 1n)$ ,  $(\gamma, 2n)$ , and  $(\gamma, 3n)$ , is widely used in both fundamental and applied research including traditional studies of the Giant Dipole Resonance (GDR) excitation and decay mechanisms (configurational and isospin splitting, competition between statistical and direct processes in GDR decay channels, sum rule exhaustion, etc.) as well as in various applications such as beam luminosity monitoring in ultra-relativistic heavy-ion colliders [1]. Energy thresholds of the  $(\gamma, 1n)$ ,  $(\gamma, 2n)$ ,  $(\gamma, 3n)$ , ... reactions  $B1n$ ,  $B2n$ ,  $B3n$ , ... are relatively close and therefore there are ranges of the incident photon energy where there is a competition of two or three open reaction channels.

The majority of data under discussion were obtained using the method of outgoing neutron detection where the summed photoneutron yield cross section

$$\sigma(\gamma, Sn) = \sigma[(\gamma, 1n) + 2(\gamma, 2n) + 3(\gamma, 3n) + \dots] \quad (1)$$

was measured directly. Since the neutron from the  $(\gamma, 1n)$  reaction is detected once, two neutrons from the  $(\gamma, 2n)$  reaction are detected twice, and so on, the cross sections of partial reactions appear in  $\sigma(\gamma, Sn)$  with corresponding multiplicity factors. Therefore, to decompose  $\sigma(\gamma, Sn)$  into partial reactions one need to know which reaction produced the detected neutron. This is a well-known problem of neutron multiplicity sorting.

The photoneutron yield cross section is used for estimating the total photoneutron cross section

$$\sigma(\gamma, \text{tot}) = \sigma[(\gamma, 1n) + (\gamma, 2n) + (\gamma, 3n) + \dots] = \sigma(\gamma, Sn) - \sigma(\gamma, 2n) - 2\sigma(\gamma, 3n) - \dots \quad (2)$$

This cross section for medium and heavy nuclei is close to the total photoabsorption cross section

$$\sigma(\gamma, \text{abs}) = \sigma(\gamma, \text{tot}) + \sigma(\gamma, 1p) + \sigma(\gamma, 2p) + \dots, \quad (3)$$

could be compared with TRK sum rule estimations:

$$\sigma^{\text{int}}(\gamma, \text{tot}) \approx \sigma^{\text{int}}(\gamma, \text{abs}) = \int_0^{\infty} \sigma(E) dE = 60 NZ/A \text{ MeV, mb}, \quad (4)$$

where  $Z$  and  $N$  are respectively numbers of protons and neutrons in the nucleus, and  $A = Z + N$  is the atomic mass number.

Most of the neutron yield, total photoneutron and partial photonuclear reactions cross sections were obtained using quasimonochromatic annihilation photon beams at the *National Lawrence Livermore Laboratory (USA)* and *France Centre d'Etudes Nucleaires de Saclay*. The data can be found in numerous reviews [2], Atlases [3, 4] and databases [5].

Both laboratories mentioned employed similar methods to identify reactions with different multiplicities based on the same assumption that the neutron spectra of  $(\gamma, 1n)$  and  $(\gamma, 2n)$  reactions are quite different. However the methods for neutron kinetic energy measurement used were significantly different. Complex systematic discrepancies in partial photoneutron reaction cross sections are well-known: in many cases for the same nuclei the  $(\gamma, 1n)$  reaction cross sections are noticeably larger at Saclay, but the  $(\gamma, 2n)$  cross sections vice versa are larger at Livermore and disagreements approach  $\sim 60\%$ . Fig. 1 shows the typical example of such kind disagreements for  $^{159}\text{Tb}$ .

These disagreements were the subject of special studies for several years [6–10].

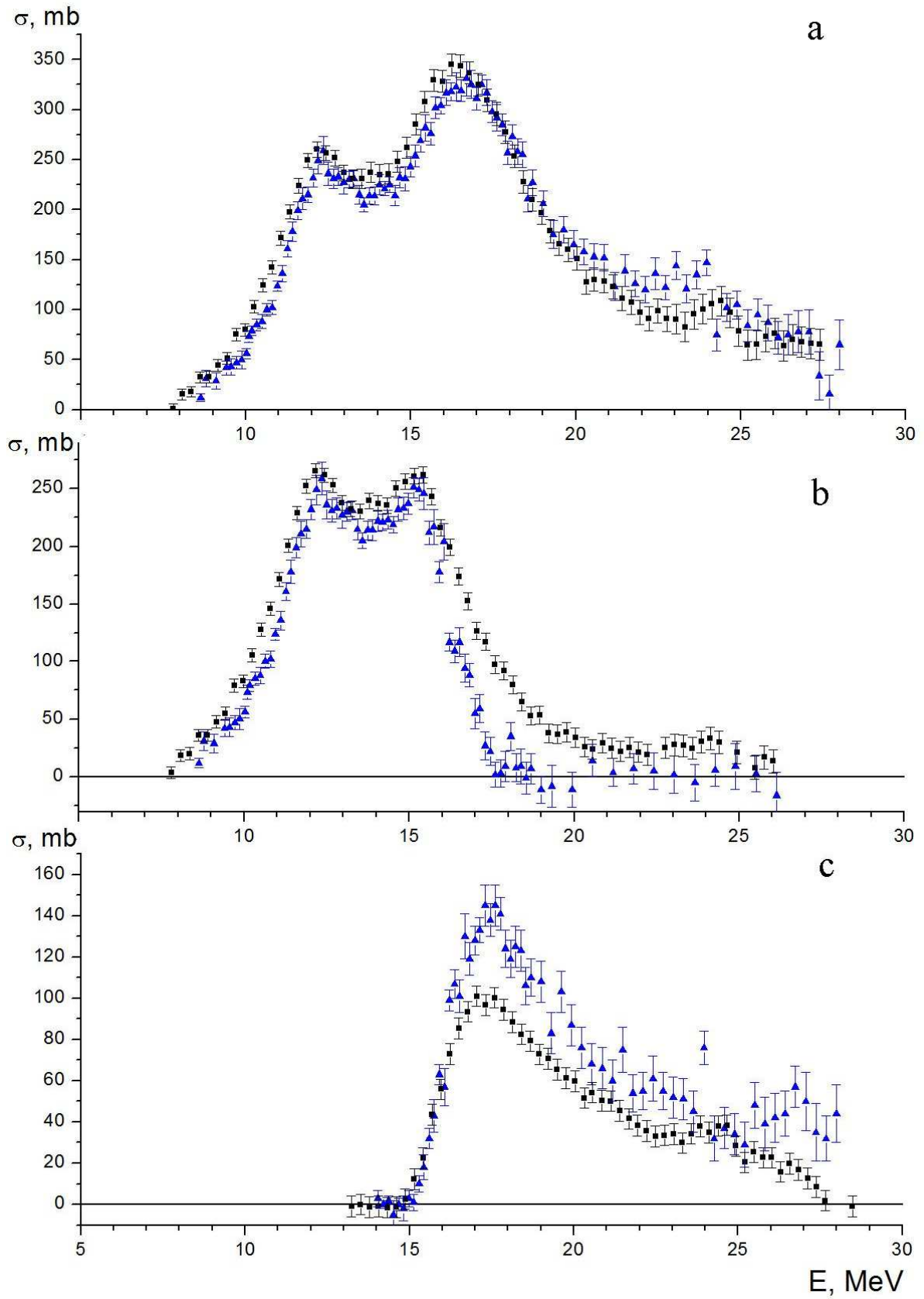


Fig. 1. The comparison of cross section data for  $^{159}\text{Tb}$  obtained using quasimonoenergetic annihilation photons in [11] – triangles and [12] – squares: a –  $\sigma(\gamma, \text{Sn})$ , b –  $\sigma(\gamma, n)$ , c –  $\sigma(\gamma, 2n)$ .

The complete systematics of integrated cross sections  $\sigma^{\text{int}}$

$$\sigma^{\text{int}} = \int_B^{E^{\text{int}}} \sigma(E) dE \quad (5)$$

has become available [9, 10] for more than 500 photoneutron yield cross section (1) data for nuclei from  $^3\text{H}$  to  $^{238}\text{U}$ . To avoid additional uncertainties related with photoneutron multiplicity, the integrated cross sections  $\sigma_{\text{syst}}^{\text{int}}$  for each nucleus were calculated for incident photon energy intervals between the thresholds B1n and B2n. The systematics of ratio

$$R_{\text{syst}}^{\text{int}} = \sigma_{\text{syst}}^{\text{int}} \text{ various} / \sigma_{\text{syst}}^{\text{int}} \text{ Livermore} \quad (6)$$

of the integrated cross section data from various laboratories to that obtained in Livermore laboratory, is shown in Fig. 2. The results shown confirm clearly that in spite of some spread of the  $R_{\text{syst}}^{\text{int}}$  values obtained in various laboratories they are concentrated near the value about 10 % – averaged value  $\langle R_{\text{syst}}^{\text{int}} \rangle = 1.12 \pm 0.24$  (one can see that Livermore data are slightly lower than others).

At the same time the situation for partial reaction cross sections is quite different. Fig. 3 shows the complete systematics of integrated cross section ratios (Saclay/Livermore)

$$R^{\text{int}}(1n) = \sigma_{\text{s}}^{\text{int}}(\gamma, 1n) / \sigma_{\text{L}}^{\text{int}}(\gamma, 1n), \quad (7)$$

$$R^{\text{int}}(2n) = \sigma_{\text{s}}^{\text{int}}(\gamma, 2n) / \sigma_{\text{L}}^{\text{int}}(\gamma, 2n) \quad (8)$$

obtained [9] for 19 nuclei ( $^{51}\text{V}$ ,  $^{75}\text{As}$ ,  $^{89}\text{Y}$ ,  $^{90}\text{Zr}$ ,  $^{115}\text{In}$ ,  $^{116,117,118,120,124}\text{Sn}$ ,  $^{127}\text{I}$ ,  $^{133}\text{Cs}$ ,  $^{159}\text{Tb}$ ,  $^{165}\text{Ho}$ ,  $^{181}\text{Ta}$ ,  $^{197}\text{Au}$ ,  $^{208}\text{Pb}$ ,  $^{232}\text{Th}$ ,  $^{238}\text{U}$ ) investigated in both laboratories. One can see that in accordance with example from Fig. 1 large disagreements between partial reaction cross sections exist:  $\langle R^{\text{int}}(1n) \rangle$  is about 1.2 but  $\langle R^{\text{int}}(2n) \rangle$  is about 0.8.

It has been suggested [6, 7] that the difference of the partial reaction cross sections originated from the procedures used to separate counts into 1n and 2n events – neutron multiplicity sorting. Using additional data employing the method of induced activity, which allows one to identify partial reactions by detecting produced final nuclei it was found [7] that Saclay  $\sigma(\gamma, 2n)$  data are significantly underestimated (and correspondingly  $\sigma(\gamma, 1n)$  overestimated) because of large systematic uncertainties. In order to resolve these problems a new approach for partial reaction cross section evaluation has been developed [13, 14].

## 1. The new method for partial reaction cross sections evaluation

Only agreed photoneutron yield cross section (1) data are used in the method developed.

Therefore the very important problem is the reliability of total photoneutron yield cross section  $\sigma(\gamma, \text{Sn})$  data. As that was found in [10] data obtained at Saclay can be used directly (without any additional normalization). At the same time data obtained at Livermore should be normalized by using discrepancy factor  $\langle R_{\text{syst}}^{\text{int}} \rangle \approx 1.12$ .

In this approach the experimental neutron yield cross section  $\sigma_{\text{exp}}(\gamma, \text{Sn})$  (1) is used only as the initial data source. To decompose that into evaluated partial reaction cross sections

$$\sigma_{\text{eval}}(\gamma, 1n) = F_{1\text{-th}} \sigma_{\text{exp}}(\gamma, \text{Sn}) = [\sigma_{\text{th}}(\gamma, 1n) / \sigma_{\text{th}}(\gamma, \text{Sn})] \sigma_{\text{exp}}(\gamma, \text{Sn}), \quad (9)$$

$$\sigma_{\text{eval}}(\gamma, 2n) = F_{2\text{-th}} \sigma_{\text{exp}}(\gamma, \text{Sn}) = [\sigma_{\text{th}}(\gamma, 2n) / \sigma_{\text{th}}(\gamma, \text{Sn})] \sigma_{\text{exp}}(\gamma, \text{Sn}), \dots \quad (10)$$

so-called transitional neutron multiplicity functions  $F_{i\text{-th}}$  are used. They are calculated within the framework of the combined photonuclear reaction model [15, 16] for all partial reactions ( $\gamma, in$ ) with definite neutron multiplicity factors  $i = 1, 2, 3, \dots$ :

$$F_{i\text{-th}} = \sigma_{\text{th}}(\gamma, in) / \sigma_{\text{th}}(\gamma, \text{Sn}) = \sigma_{\text{th}}(\gamma, in) / \sigma_{\text{th}}[(\gamma, 1n) + 2(\gamma, 2n) + 3(\gamma, 3n) + \dots]. \quad (11)$$

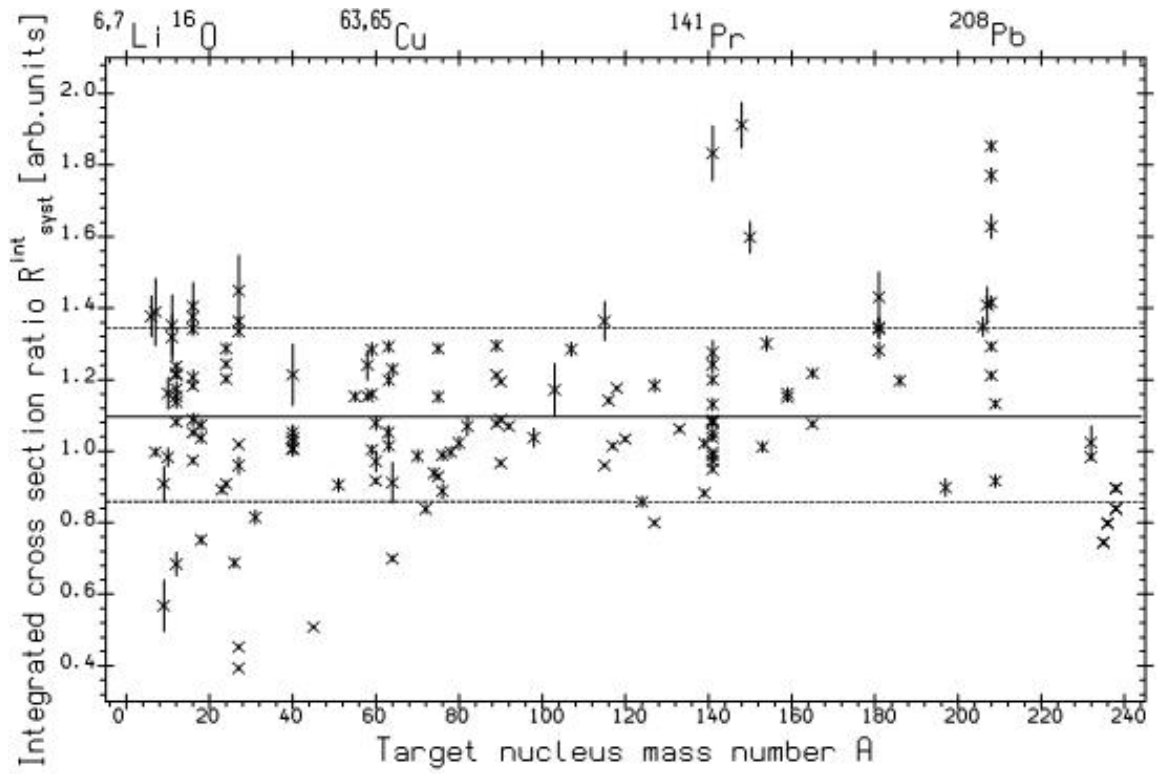


Fig. 2. The complete systematics of  $\sigma(\gamma, \text{Sn})$  reaction integrated cross section ratios  $R_{\text{syst}}^{\text{int}}$  data.

$$R^{int} = \sigma_S^{int} / \sigma_L^{int}, \text{ arb. units}$$

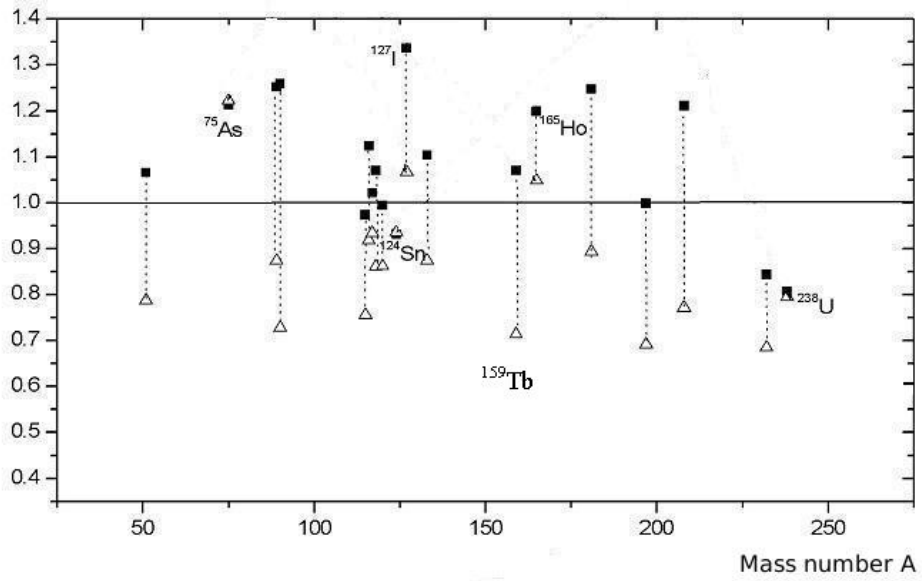


Fig. 3. The complete systematics of disagreements between data for  $\sigma(\gamma, 1n)$  and  $\sigma(\gamma, 2n)$  - the ratios of integrated cross sections  $R^{int}(1n)$  - squares and  $R^{int}(2n)$  - triangles.

Therefore, the developed approach allows one to keep the ratios of evaluated partial reaction cross sections  $\sigma_{\text{eval}}(\gamma, \text{in})$  equal to the ratios of the theoretically calculated cross sections.

It should be noted that the functions  $F_{i\text{-th}}$  calculated using the model [15, 16] consistent with calculations performed using well-known and widely used TALYS [17] and EMPIRE [18] models.

### 1.1. Criteria of the systematic uncertainties

The multiplicity functions  $F_{i\text{-th}}$  introduced in ((9)–(11)) allow us to evaluate the systematic uncertainties in partial reactions cross sections.

According to its definition (11)  $F_{1\text{-th}}$  is the ratio of  $\sigma(\gamma, 1n)$  to a sum [ $\sigma(\gamma, 1n) + 2(\gamma, 2n) + 3(\gamma, 3n)$ ] and, therefore, can never be greater than 1.00;  $F_{2\text{-th}}$  is the ratio of  $\sigma_{\text{th}}(\gamma, 2n)$  to a sum [ $\sigma_{\text{th}}(\gamma, 1n) + 2\sigma_{\text{th}}(\gamma, 2n) + 3\sigma_{\text{th}}(\gamma, 3n)$ ] and, therefore, can never be greater than 0.50; correspondingly  $F_{3\text{-th}}$  is the ratio of  $\sigma_{\text{th}}(\gamma, 3n)$  to a sum [ $\sigma_{\text{th}}(\gamma, 1n) + 2\sigma_{\text{th}}(\gamma, 2n) + 3\sigma_{\text{th}}(\gamma, 3n)$ ] and, therefore, never can be greater than 0.33, and so on.

Functions  $F_{1\text{-th}}$  and  $F_{2\text{-th}}$  calculated [15, 16] for  $^{94}\text{Zr}$  [19] are shown by lines in Fig. 4a, b. As it follows from definitions (11) the natural and physically believable energy dependences of  $F_{1,2\text{-th}}$  should have the following energy dependencies:

- Below the  $(\gamma, 2n)$  reaction threshold B2n only the  $(\gamma, 1n)$  reaction is possible and therefore  $F_{1\text{-th}} = 1$ ,  $F_{2\text{-th}} = 0$ ;
- Above B2n both  $(\gamma, 1n)$  and  $(\gamma, 2n)$  reactions are possible,  $F_{2\text{-th}}$  increases approaching the theoretical limit of 0.50, but never reaching it because of a high-energy part in  $\sigma_{\text{th}}(\gamma, 1n)$ ;
- Above the B3n threshold the  $(\gamma, 3n)$  reaction is also possible,  $F_{2\text{-th}}$  decreases due to a  $3\sigma_{\text{th}}(\gamma, 3n)$  term in denominator of (11).

The energy dependencies (Fig. 4 a, b) of functions  $F_{i\text{-exp}} = \sigma_{\text{exp}}(\gamma, \text{in})/\sigma_{\text{exp}}(\gamma, \text{Sn})$ , obtained using cross sections on  $^{94}\text{Zr}$  [19], are definitely different from the dependencies of  $F_{i\text{-th}}$  functions: in the energy range  $\sim 21.5 - 28.0$  MeV there are many  $F_{1\text{-exp}}$  physically forbidden negative values and physically forbidden values  $F_{2\text{-exp}} > 0.50$ . This clear correlation means that multiplicity sorting [19] has been performed incorrectly because of erroneous addition of extra neutrons with multiplicity two (as a matter of fact, subtracted from multiplicity–one neutrons).

In a series of works [16, 17, 20–22, 23] functions  $F_{1,2,3}$  were found out for a large number of cross sections ( $^{90,91,94}\text{Zr}$  [19],  $^{115}\text{In}$ ,  $^{112,114,116,117,118,119,120,122,124}\text{Sn}$  [24],  $^{159}\text{Tb}$  [11],  $^{181}\text{Ta}$  [25],  $^{188,189}\text{Os}$  [26],  $^{208}\text{Pb}$  [27]).

Various data obtained for four isotopes ( $^{94}\text{Zr}$ ,  $^{118}\text{Sn}$ ,  $^{159}\text{Tb}$  and  $^{181}\text{Ta}$ ) will be described as typical examples. The systematics of evaluated data is presented in Annex.

### 1.2. Evaluated partial photoneutron reaction cross sections

Evaluated cross sections in many cases differ from the experimental ones noticeably. Fig. 5 shows as an example of such deviations of evaluated data from experimental data [11] and [12] for two main partial reactions  $(\gamma, 1n)$  and  $(\gamma, 2n)$  on  $^{159}\text{Tb}$ . One can see that evaluated  $\sigma_{\text{eval}}^{\text{int}}(\gamma, 1n)$  [20] is about 20% smaller than data [12] but 20% larger than data [11],  $\sigma_{\text{eval}}^{\text{int}}(\gamma, 2n)$  is 15% larger than [12] data but 20% smaller than the [11]. Thus, the evaluated ratio  $\sigma_{\text{eval}}^{\text{int}}(\gamma, 2n)/\sigma_{\text{eval}}^{\text{int}}(\gamma, 1n)$ , which plays an important role in estimation of probabilities of different physical processes, obtained using our evaluated data is about 30% larger in comparison to data [12] and 30% smaller in comparison to data [11].

The most important consequence of the differences obtained is that those are reflected in the values of the total photoneutron reaction cross section (2) directly connected with total photoabsorption cross section (3).

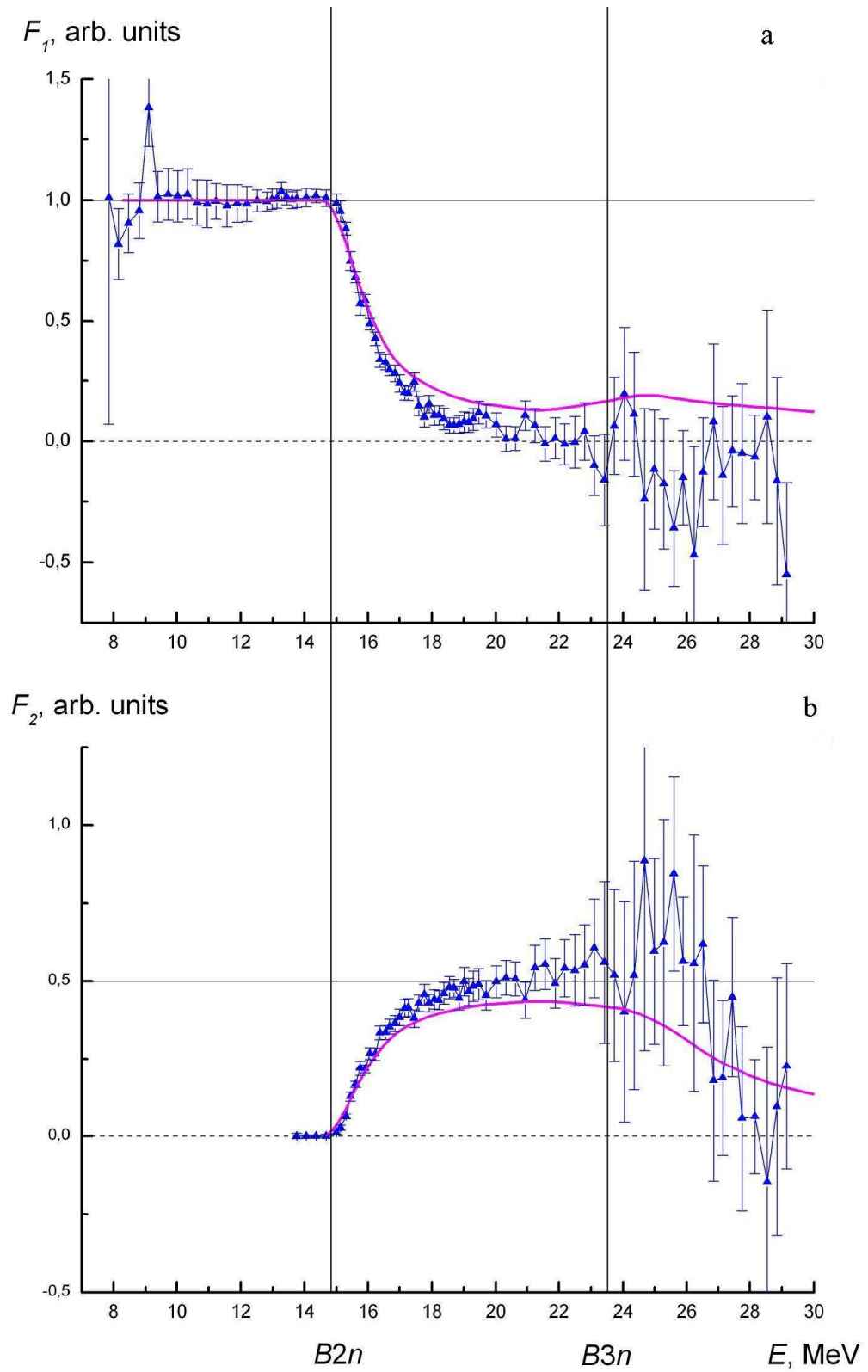


Fig. 4. The comparison of experimental ([19] – triangles) and theoretical ([15], [16] – lines) neutron multiplicity functions  $F_1$  (a) and  $F_2$  (b) for  $^{94}\text{Zr}$ .

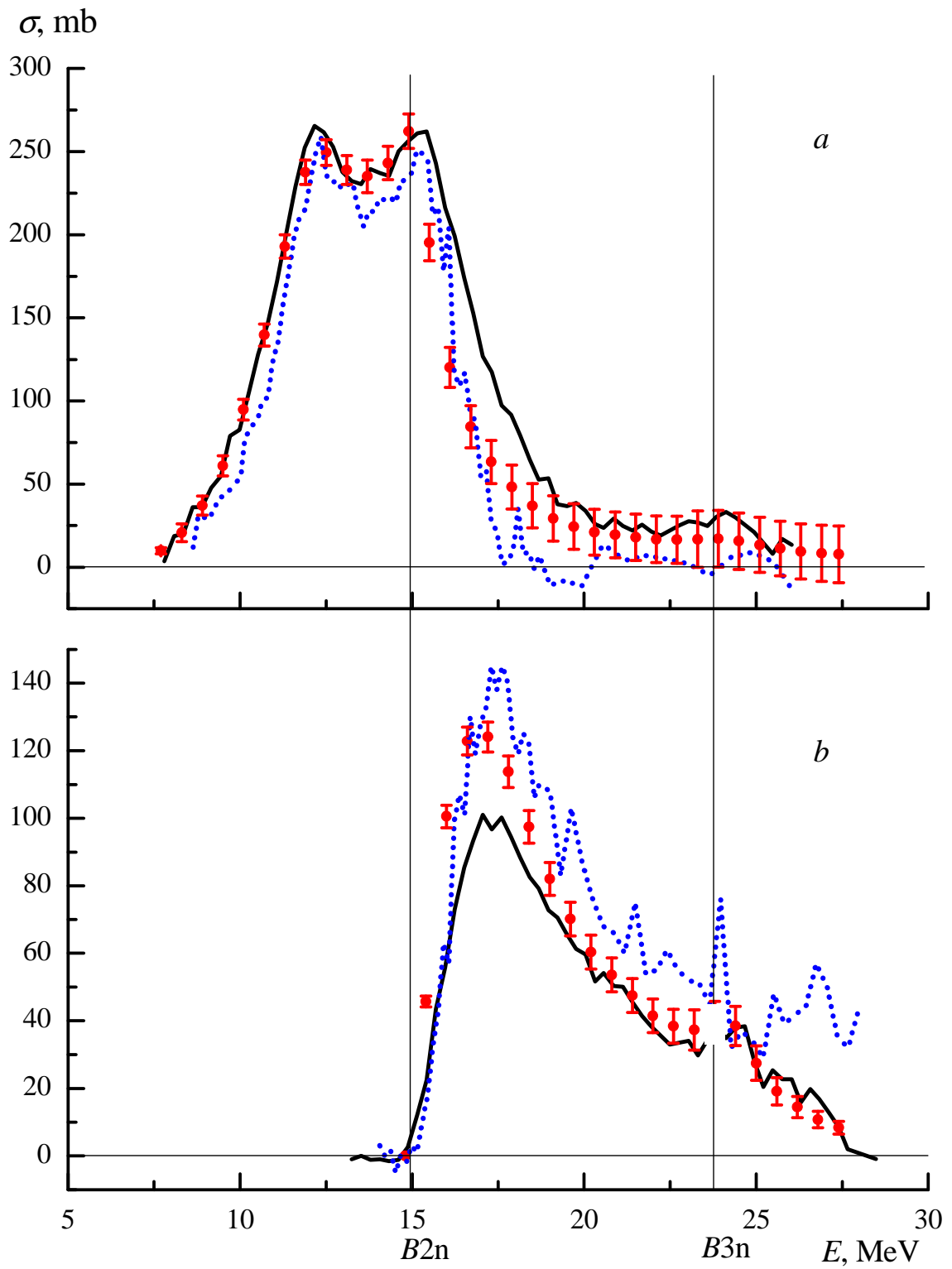


Fig. 5. The comparison of evaluated ([19], dots) and experimental ([11] – dash and [12] – line) photonuclear reaction cross sections for  $^{159}\text{Tb}$ :  
 a –  $\sigma(\gamma, 1n)$ ;  
 b –  $\sigma(\gamma, 2n)$ .

## 2. Reliability of evaluated data from comparison with alternative experiments results

The proposed new approach gives to one possibility to reduce systematic uncertainties of the methods of neutron multiplicity sorting in evaluated partial reaction cross sections. Therefore evaluated data can be compared with a few results obtained using alternative experimental methods free from such kind uncertainties.

### 2.1. Comparison with the results of induced activity experiment

As it was mentioned above one of such alternative methods is that of induced activity in which the studied reaction is identified through detection of the residual nucleus rather than outgoing neutrons. Since the final nuclei of the  $(\gamma, 1n)$ ,  $(\gamma, 2n)$ , and  $(\gamma, 3n)$  reactions are different the method of induced activity has no problems with their separation and can be used to obtain partial reaction yields directly.

With the aim of such kind comparison in details special measurements were performed [28] using the photon beam of a race-track microtron with maximal electron energy 65 MeV. Reaction yields

$$Y(E_{\max}) = \alpha \int_B^{E_{\max}} W(E_{\max}, E) \sigma(E) dE, \quad (12)$$

where  $W(E_{\max}, E)$  is the bremsstrahlung spectrum with end-point energy  $E_{\max} = 65$  MeV,  $B$  is the corresponding reaction threshold, were simultaneously measured [28] in a single experiment for reactions  $(\gamma, 1n)$ ,  $(\gamma, 2n)$ ,  $(\gamma, 3n)$ ,  $(\gamma, 4n)$ ,  $(\gamma, 5n)$ ,  $(\gamma, 6n)$ , and  $(\gamma, 7n)$  on  $^{181}\text{Ta}$  using a high-purity HPGe detector.

In table 1 corresponding the ratios of yields (12) for pairs of reactions  $Y(\gamma, 2n)/Y(\gamma, 1n)$  and the ratios of integrated cross sections (5)  $\sigma^{\text{int}}(\gamma, 2n)/\sigma^{\text{int}}(\gamma, 1n)$  obtained for  $^{181}\text{Ta}$  are compared.

Table 1. The comparison of ratios of reaction yields  $Y$  (12) and integrated cross sections  $\sigma^{\text{int}}$  (5) obtained for experimental (according to [3]) and evaluated data for  $^{181}\text{Ta}$  for  $E^{\text{int}} = 65$  MeV.

Ratio	Experiment			Evaluation
	Saclay [12]	Livermore [11]	Activity [28]	Our data [20]
$\sigma^{\text{int}}(\gamma, 2n)/\sigma^{\text{int}}(\gamma, 1n)$	0.36 = 797/2190	0.67 = 887/1316		0.49 = 958/1956
$Y(\gamma, 2n)/Y(\gamma, 1n)$	0.24	0.42	0.34 (7)	0.33

The presented results clearly show that the ratios  $\sigma^{\text{int}}(\gamma, 2n)/\sigma^{\text{int}}(\gamma, 1n)$  [12] are certainly underestimated (0.36), while ratios [11] are overestimated (0.67) in comparison with our evaluation (0.49). The same inconsistency can be seen for yield ratios  $Y(\gamma, 2n)/Y(\gamma, 1n)$ : correspondingly 0.24 and 0.42 versus 0.33.

Data evaluated in the frame of new proposed approach agree well with activity data [28] (0.33 versus 0.34).

### 2.2. The comparison of evaluated data with the results of modern experiment using quasimonochromatic laser-Compton scattering $\gamma$ -rays

New advanced gamma-ray sources using laser-Compton scattering were built recently in various laboratories. Quasimonochromatic photons are used in studies of photonuclear reactions in

different energy ranges with priority of obtaining accurate data for  $(\gamma, 1n)$  reactions cross sections near thresholds. A large amount of data was obtained using this technique at the National Institute of Advanced Industrial Science and Technology (Japan) [29], including reaction cross sections on the nuclei, that are subjected to our evaluations.

Fig. 6 shows the comparison of the  $^{118}\text{Sn}(\gamma, 1n)^{117}\text{Sn}$  reaction cross section measured using laser-Compton scattering [29] for neutrons with multiplicity equal to 1 with quasimonoenergetic annihilation photon experimental data [19, 30] and evaluated cross section [13]. One can see that the evaluated cross section is in agreement with the laser-Compton scattering experiment result. At the same time quasimonoenergetic annihilation photons data are underestimated/overestimated, which is consistent with the previous discussion.

### 3. Possible reasons for evaluated and experimental data distinctions

As it was said above the neutron multiplicity determination methods used were based on the assumption that the energy of a single neutron from the  $(\gamma, 1n)$  reaction is noticeably higher than energies of the  $(\gamma, 2n)$  reaction neutrons.

But as it was shown the degree of discrepancies between various quasimonoenergetic annihilation photon experiments data as well as between experimental and newly evaluated cross sections in  $1n$ ,  $2n$ , and  $3n$  channels depend on the energy of photons and, therefore, on the energy spectra of outgoing neutrons. It means that the relation between the energy of a neutron and its multiplicity could be in fact more complex.

A special study [28] showed that mean energy of the 1st neutron from the reaction  $^{181}\text{Ta}(\gamma, 2n)^{179}\text{Ta}$  is much larger than that of the 2nd neutron (for example, when the photon energy is 25 MeV the mean energy of the 1st neutron is 4.0 MeV, of the 2nd neutron – 1.4 MeV). Theoretical calculations [28] of neutron energy spectra in the  $(\gamma, 1n)$  and  $(\gamma, 2n)$  reactions on  $^{159}\text{Tb}$  and  $^{181}\text{Ta}$  within the framework of the model [15, 16] used in our approach show that in the photon energy ranges  $E_\gamma < 12.2 \text{ MeV} < B_{2n} = 14.2 \text{ MeV}$  and  $E_\gamma < 19.2 \text{ MeV} > B_{2n}$  the shapes of neutron energy spectra are close.

Additionally, as it has been already pointed before the actual situation could be more complicated because in a  $(\gamma, 1n)$  reaction after escape of a single neutron and in  $(\gamma, 2n)$  and  $(\gamma, 3n)$  reactions after escape of the first chance neutron the same nucleus is formed. Moreover, the same nucleus is formed after escape of the first chance neutron in reactions  $(\gamma, 1n1p)$ ,  $(\gamma, 2n1p)$ , ..., which can also have low thresholds.

It must be stressed once again that in quasimonoenergetic annihilation photons experiments with direct detection of outgoing neutrons the proton channels were not considered at all. In many cases in these experiments the reported value  $\sigma_{\text{exp}}(\gamma, 1n)$  was in fact the sum  $\sigma_{\text{exp}}(\gamma, 1n) + \sigma_{\text{exp}}(\gamma, 1np)$ , and  $\sigma_{\text{exp}}(\gamma, 2n)$  – the sum  $\sigma_{\text{exp}}(\gamma, 2n) + \sigma_{\text{exp}}(\gamma, 2np)$ , and so on.

The new developed approach to evaluation of partial photoneutron reaction cross sections properly takes into account the proton decay channels ((9)–(11)) as  $\sigma_{\text{th}}(\gamma, \text{Sn})$  used for determination of the  $F_{1,2,3}$  functions includes  $\sigma(\gamma, 1np)$ :

$$\sigma_{\text{th}}(\gamma, \text{Sn}) = \sigma_{\text{th}}[(\gamma, 1n) + (\gamma, 1np) + 2(\gamma, 2n) + 3(\gamma, 3n) + \dots]. \quad (13)$$

Thus, the main reason of disagreements between experimental and evaluated cross sections is a very complex and indirect relationship between neutron kinetic energy and its multiplicity.

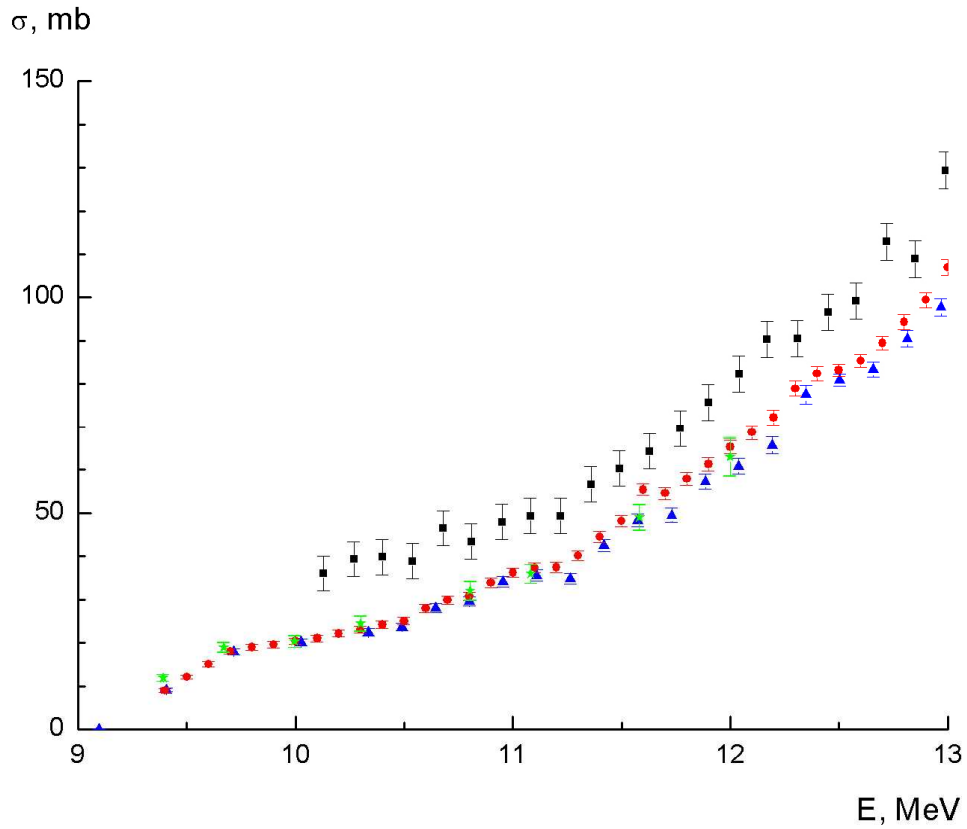


Fig. 6. The comparison of data for  $^{118}\text{Sn}(\gamma, 1n)^{117}\text{Sn}$  reaction cross section near threshold obtained by various ways: triangles [19] and squares [30] are quasimonoenergetic annihilation photons data, stars – laser-Compton scattering data [29], circles – our evaluated data [13].

## 4. Summary and conclusions

New criteria  $F_i = \sigma(\gamma, in)/\sigma(\gamma, Sn)$  of systematic uncertainties presence in photoneutron partial reaction cross sections presence were proposed.

New method was developed for evaluation of partial reaction cross sections. In that experimental neutron yield reaction cross section  $\sigma_{exp}(\gamma, Sn)$  independent on the shortcomings of the neutron multiplicity sorting methods is decomposed into partial reaction cross sections using the combined photonuclear reaction model equations.

On the base of various results obtained for isotopes  $^{94}\text{Zr}$ ,  $^{118}\text{Sn}$ ,  $^{159}\text{Tb}$  and  $^{181}\text{Ta}$  that was shown that evaluated data are not agree with data obtained in quasimonoenergetic annihilation photons experiments via neutron multiplicity sorting but agree with results obtained using the induced activity methods.

Therefore much experimental data on partial photoneutron reaction cross sections should be re-analyzed and/or re-evaluated.

Data obtained within the framework of new method developed for evaluation of partial reaction cross sections for nuclei  $^{91,94}\text{Zr}$ ,  $^{115}\text{In}$ ,  $^{159}\text{Tb}$ ,  $^{181}\text{Ta}$ ,  $^{188,189,190,192}\text{Os}$ , and  $^{208}\text{Pb}$  are presented in Annex.

## Acknowledgements

The work was partially supported by Russia Foundation for Basic Research (RFBR) NN 09–02–00368 and 13–02–00124.

Authors acknowledge very much Drs. M.A.Makarov, T.S.Polevich, and K.A.Stopani for help in data obtaining, processing and presentation.

## References

1. Pshenichnov I.A., Karpechev E.V., Kurepin A.B., Mishustin I.N. 2011. Yadernaya Fizika. 74. 1.
2. Berman B.L., Fultz S.S. 1975. Rev. Mod. Phys. 47. 713.
3. Dietrich S S., Berman B.L. 1988. Atom. Data and Nucl. Data Tables. 38. 199.
4. Varlamov A V, Varlamov V V, Rudenko D S, Stepanov M E. 1999. INDC(NDS)–394, IAEA NDS, Vienna, Austria
5. Russia Lomonosov Moscow State University Skobeltsyn Institute of Nuclear Physics Centre for Photonuclear Experiments Data database “Nuclear Reaction Database (EXFOR)”, URL: <http://cdfc.sinp.msu.ru/exfor/index.php>  
USA National Nuclear Data Center database “CSISRS and EXFOR Nuclear reaction experimental data”, URL: <http://www.nndc.bnl.gov/exfor/exfor00.htm>
6. Woly nec E., Martinez A.R.V., Gouffon P. et al. 1984. Phys.Rev. C29. 1137.
7. Woly nec E., Martins M.N. 1987. Revista Brasileira Fisica. 17. 56.
8. Berman B.L., Pywell R.E., Dietrich S.S. et al. 1987. Phys.Rev. C36. 1286.
9. Varlamov V.V., Peskov N.N., Rudenko D.S., Stepanov M.E. 2004, INDC(CCP)–440, IAEA NDS, Vienna, Austria, p. 37.
10. V.V.Varlamov, B.S.Ishkhanov. Study of Consistency Between  $(\gamma, xn)$ ,  $[(\gamma, n) + (\gamma, np)]$  and  $(\gamma, 2n)$  Reaction Cross Sections Using Data Systematics. Vienna, Austria. INDC(CCP)-433, IAEA NDS, Vienna, Austria, 2002.
11. Bramblett R.L., Caldwell J.T., Harvey R.R., Fultz S.C. 1964. Phys.Rev. 133. B869.
12. Bergere R., Beil H., Veysiere A. 1968. Nucl.Phys. A121. 463.
13. Varlamov V.V, Ishkhanov B.S, Orlin V.N., Chetvertkova V.A. 2010. Bull. Rus. Acad. Sci. 74. 883.
14. Varlamov V.V., Ishkhanov B.S., Orlin V.N., Troshchiev S.Yu. 2010. Bull. Rus. Acad. Sci. 74. 842.

15. Ishkhanov B.S. and Orlin V.N. 2007. Phys. Part. Nucl. 38. 232.
16. Ishkhanov B.S. and Orlin V.N. 2008. Phys. Atom. Nucl. 71. 493.
17. Koning A.J. et al. 2007 Proc. Int. Conf. on Nuclear Data for Science and Technology (Nice, France) vol 1 (2008 CEA EDP Sciences) p. 211.
18. Chadwick M.B. et al. 1991. Phys. Rev. C44. 814.
19. Berman B.L., Caldwell J.T., Harvey R.R. et al. 1967. Phys. Rev. 162. 1098.
20. Varlamov V.V., Ishkhanov B.S., Orlin V.N., Polevich T.S., Stepanov M.E. 2011. MSU SINP Preprint–5/869.
21. Varlamov V.V., Orlin V.N., Peskov N.N., Polevich T.S. 2012. MSU SINP Preprint–1/879.
22. Varlamov V.V., Ishkhanov B.S., Orlin V.N. 2012. Phys. Atom. Nucl. 75. 1339.
23. Varlamov V.V., Ishkhanov B.S., Orlin V.N., Sopov A.V. 2010. MSU SINP Preprint–8/864.
24. Fultz S.C., Berman B.L., Caldwell J.T. et al. 1969. Phys. Rev. 186. 1255.
25. Bramblett R.L., Caldwell J.T., Auchampaugh G.F. et al. 1963. Phys. Rev. 129. 2723.
26. Berman B.L., Faul D.D., Alvarez R.A. et al. 1979. Phys. Rev. C19. 1205.
27. Harvey R.R., Caldwell J.T., Bramblett R.L. et al. 1964. Phys. Rev. 136. B126.
28. Ishkhanov B S, Orlin V N and Troshchiev S Yu. 2012. Phys. Atom. Nucl. 75. 253.
29. Utsunomiya H., Goriely S., Kamata M. et al. 2011. Phys. Rev. C84. 055805.
30. Lepretre A., Beil H., Bergere R. et al. 1974. Nucl. Phys. A219. 39.
31. Varlamov V.V., Orlin V.N., Peskov N.N., Stepanov M.E. 2013. Bull. Rus. Acad. Sci. 77. 388.
32. Russia Lomonosov Moscow State University Skobeltsyn Institute of Nuclear Physics Centre for Photonuclear Experiments Data database “Nuclear Reaction Database (EXFOR)”,  
URL: <http://cdfe.sinp.msu.ru/exfor/index.php>  
USA National Nuclear Data Center database “CSISRS and EXFOR Nuclear reaction experimental data”,  
URL: <http://www.nndc.bnl.gov/exfor/exfor00.htm>  
IAEA Nuclear Data Section “Experimental Nuclear Reaction Data (EXFOR)”,  
URL: <http://www-nds.iaea.org/exfor/exfor.htm>
32. Veysiere A., Beil H., Bergere R., Carlos P., Lepretre A. 1970. Nucl.Phys. A159. 561.

## Annex

Systematics of photonuclear reactions cross sections evaluated using new proposed method

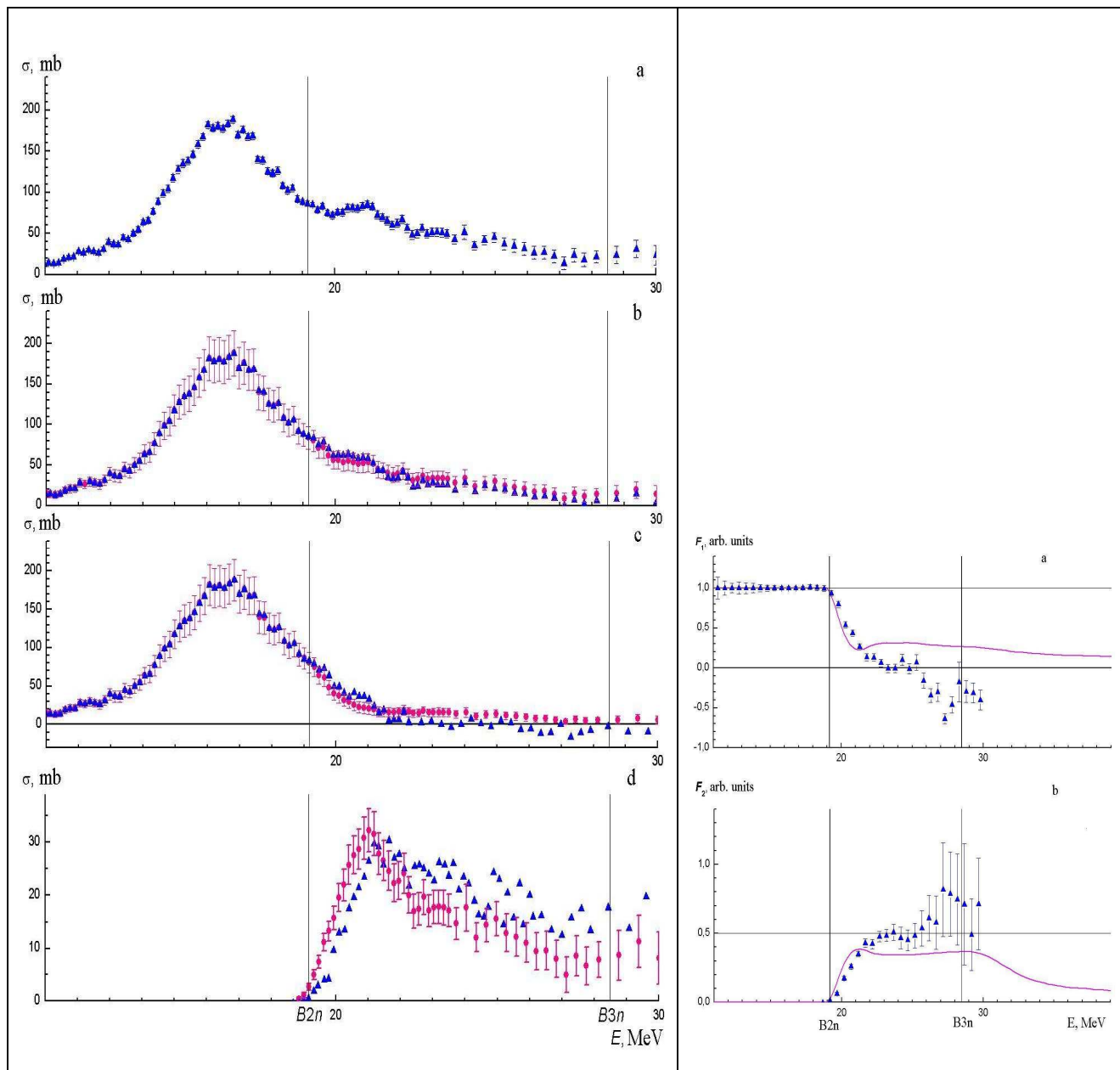


Fig. 7. Evaluated cross sections and transitional neutron multiplicity functions for  $^{91}\text{Zr}$ .  
 Left: evaluated (dots) and experimental ([19] – triangles) photonuclear reaction cross sections (a –  $\sigma(\gamma, Sn)$ , b –  $\sigma(\gamma, \text{tot})$ , c –  $\sigma(\gamma, n)$ , d –  $\sigma(\gamma, 2n)$ ).  
 Right: experimental ([19] – triangles) and theoretical ([15, 16] – lines) multiplicity functions  $F_1$  (a) and  $F_2$  (b).

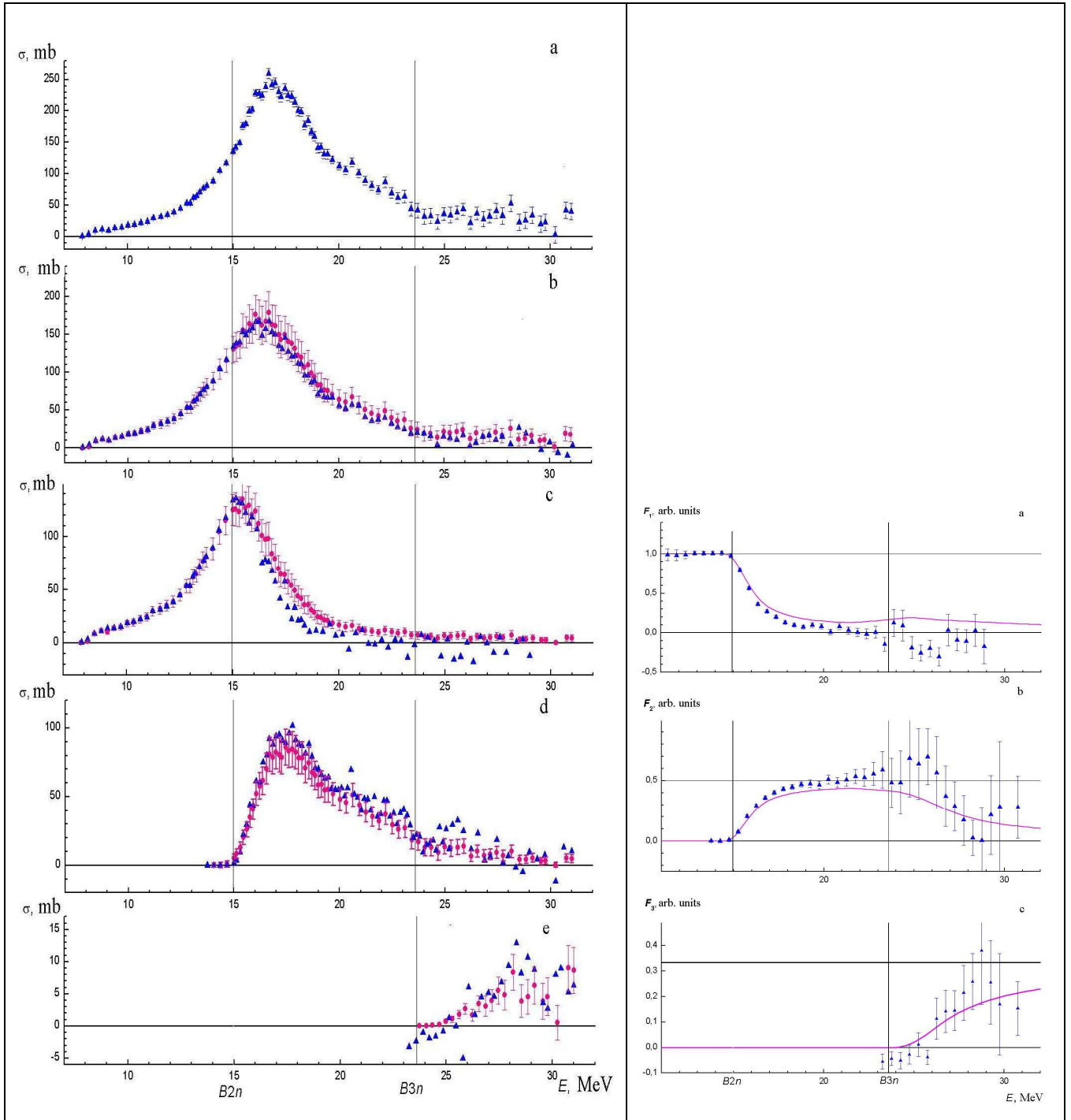


Fig. 8. Evaluated cross sections and transitional neutron multiplicity functions for  $^{94}\text{Zr}$ .  
 Left: evaluated (dots) and experimental ([19] – triangles) photonuclear reaction cross sections (a –  $\sigma(\gamma, \text{Sn})$ , b –  $\sigma(\gamma, \text{tot})$ , c –  $\sigma(\gamma, n)$ , d –  $\sigma(\gamma, 2n)$ , e –  $\sigma(\gamma, 3n)$ ).  
 Right: experimental ([19] – triangles) and theoretical ([15, 16] – lines) multiplicity functions  $F_1$  (a),  $F_2$  (b) and  $F_3$  (c).

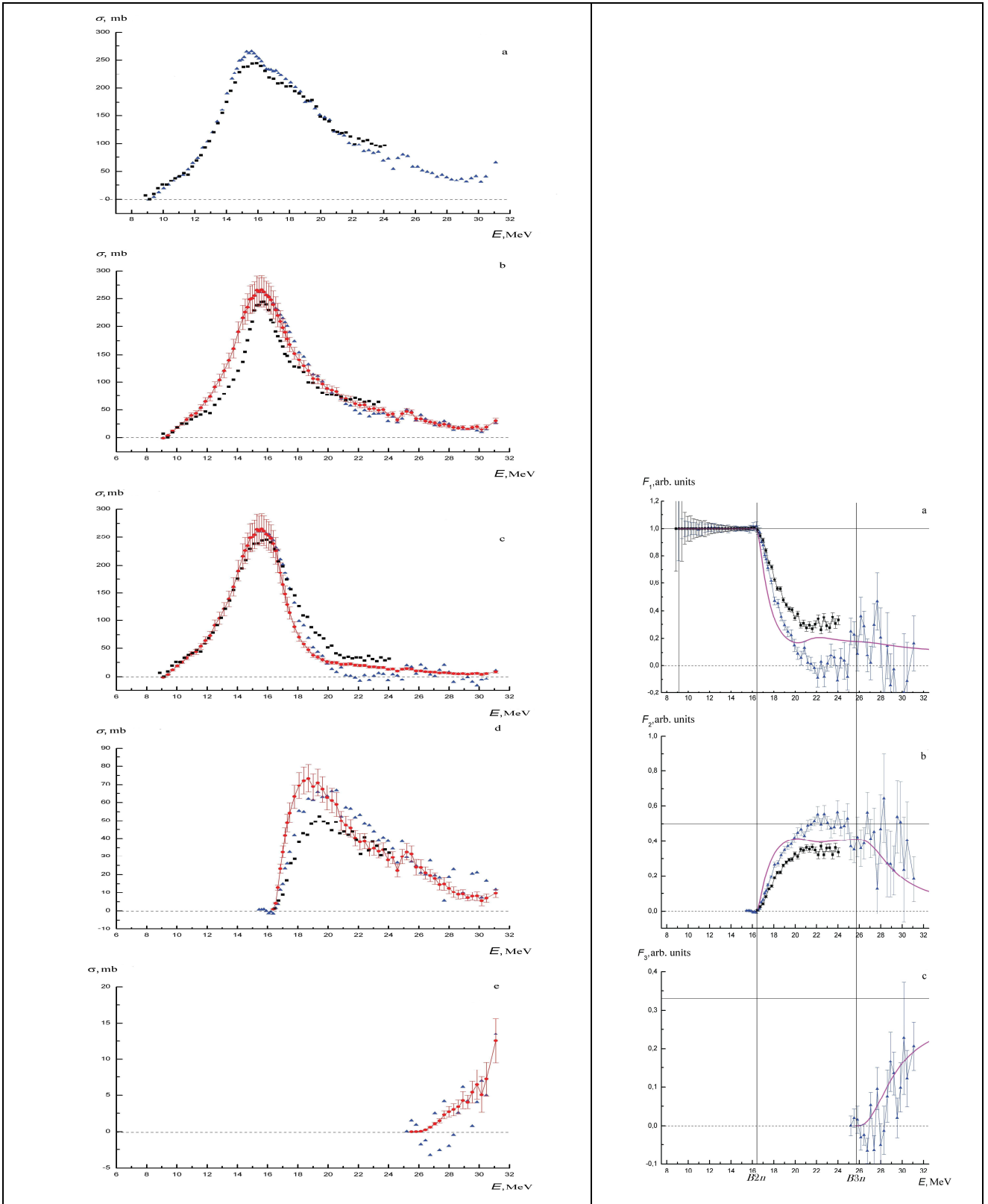


Fig. 9. Evaluated cross sections and transitional neutron multiplicity functions for  $^{115}\text{In}$ . Left: evaluated ([31, M0863] – dots) and experimental ([24] – triangles, [30] – squares) photonuclear reaction cross sections (a –  $\sigma(\gamma, \text{Sn})$ , b –  $\sigma(\gamma, \text{tot})$ , c –  $\sigma(\gamma, n)$ , d –  $\sigma(\gamma, 2n)$ , e –  $\sigma(\gamma, 3n)$ ); M0863 is the number of correspondent data set in database [32]. Right: experimental ([24] – triangles, [30] – squares) and theoretical ([15, 16] – lines) multiplicity functions  $F_1$  (a),  $F_2$  (b) and  $F_3$  (c).

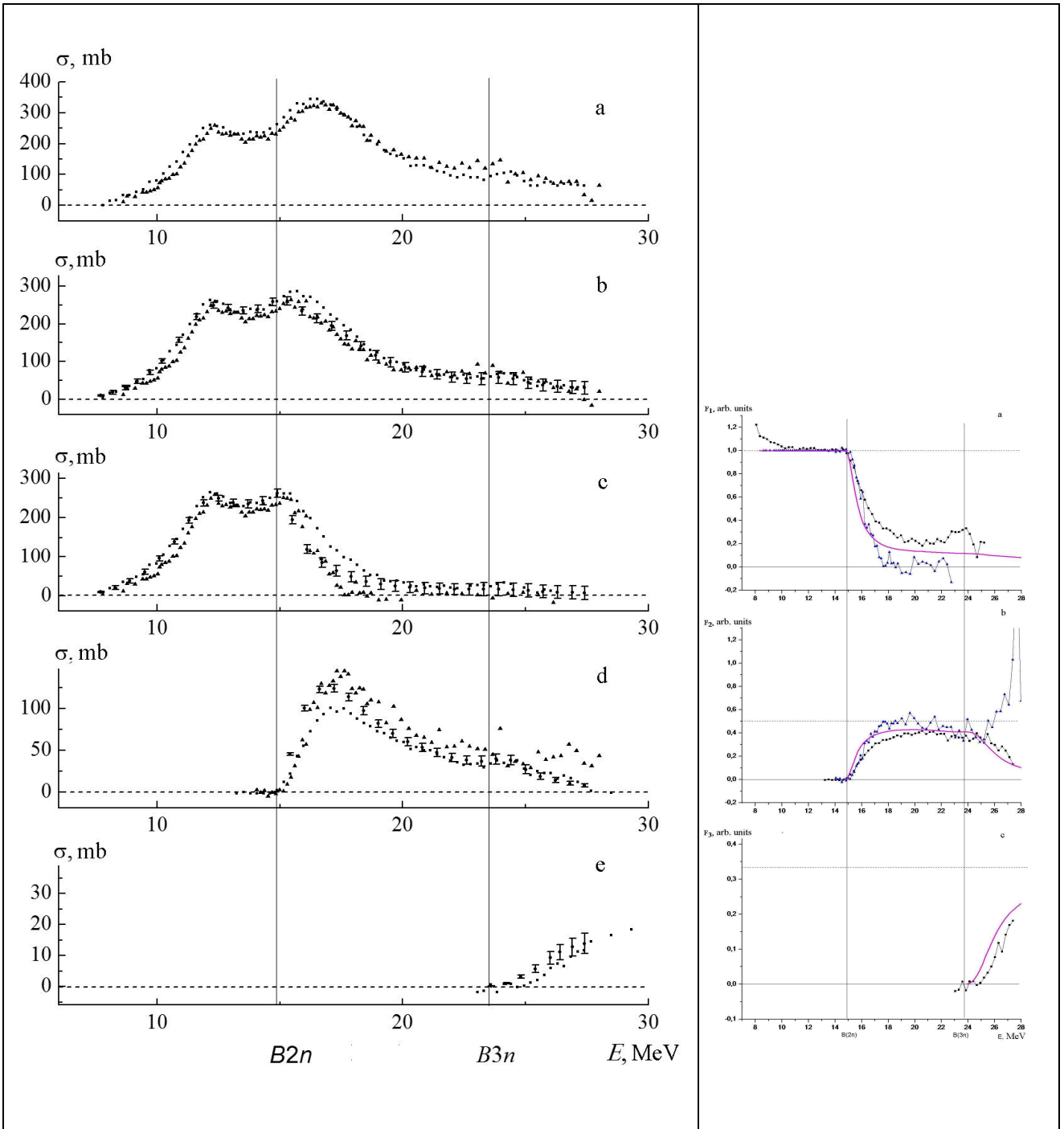


Fig. 10. Evaluated cross sections and transitional neutron multiplicity functions for  $^{159}\text{Tb}$ .  
 Left: evaluated ([20, M0831] – dots) and experimental ([11] – triangles, [12] – squares) photonuclear reaction cross sections (a –  $\sigma(\gamma, Sn)$ , b –  $\sigma(\gamma, tot)$ , c –  $\sigma(\gamma, n)$ , d –  $\sigma(\gamma, 2n)$ , e –  $\sigma(\gamma, 3n)$ ); M0831 is the number of correspondent data set in database [32].  
 Right: experimental ([11] – triangles, [12] – squares) and theoretical ([15, 16] – lines) multiplicity functions  $F_1$  (a),  $F_2$  (b) and  $F_3$  (c).

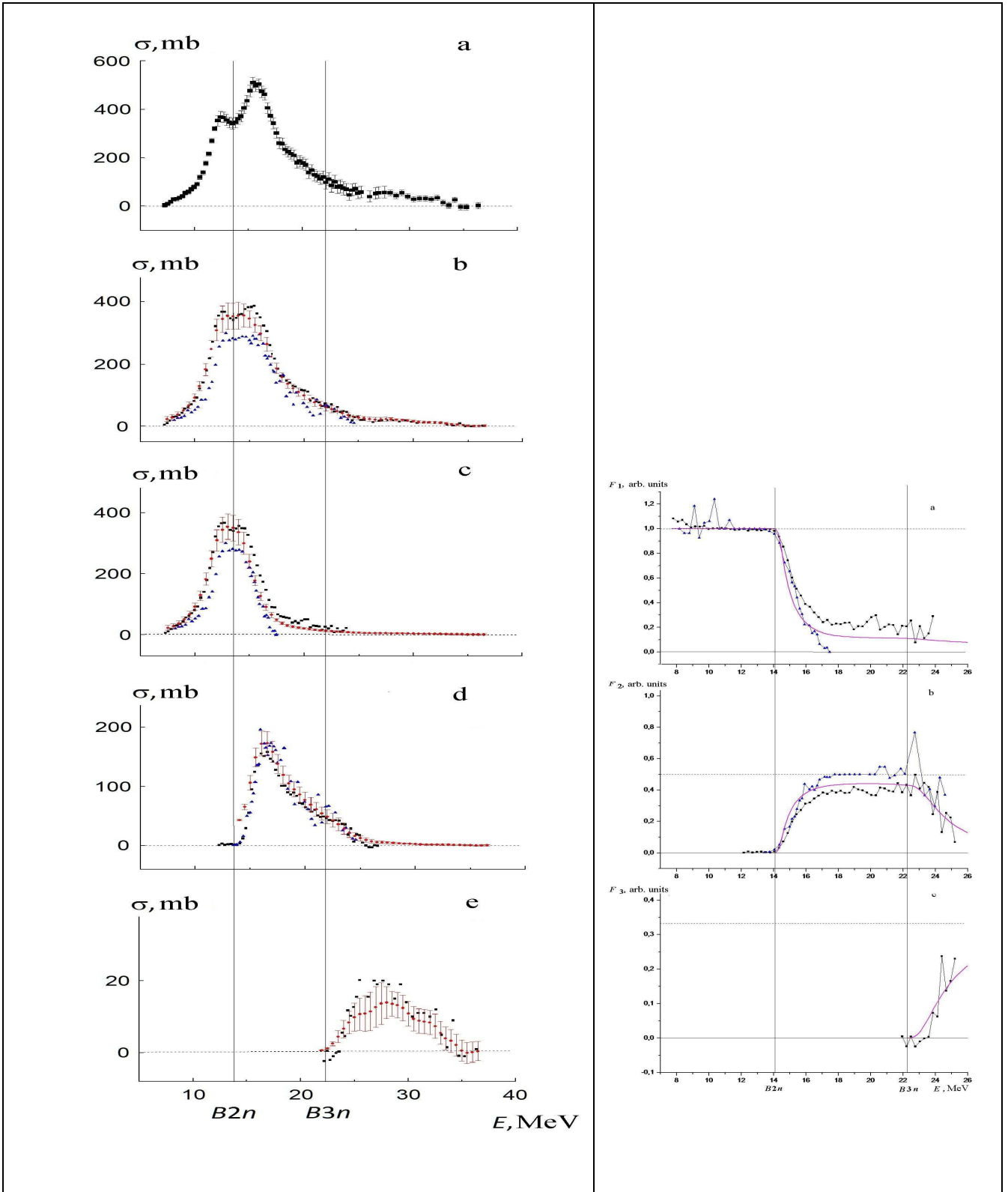


Fig. 11. Evaluated cross sections and transitional neutron multiplicity functions for  $^{181}\text{Ta}$ .  
 Left: evaluated ([21, M0850] – dots) and experimental ([25] – triangles, [12] – squares) photonuclear reaction cross sections (a –  $\sigma(\gamma, Sn)$ , b –  $\sigma(\gamma, tot)$ , c –  $\sigma(\gamma, n)$ , d –  $\sigma(\gamma, 2n)$ , e –  $\sigma(\gamma, 3n)$ ); M0850 is the number of correspondent data set in database [32].  
 Right: experimental ([25] – triangles, [12] – squares) and theoretical ([15, 16] – lines) multiplicity functions  $F_1$  (a),  $F_2$  (b) and  $F_3$  (c).

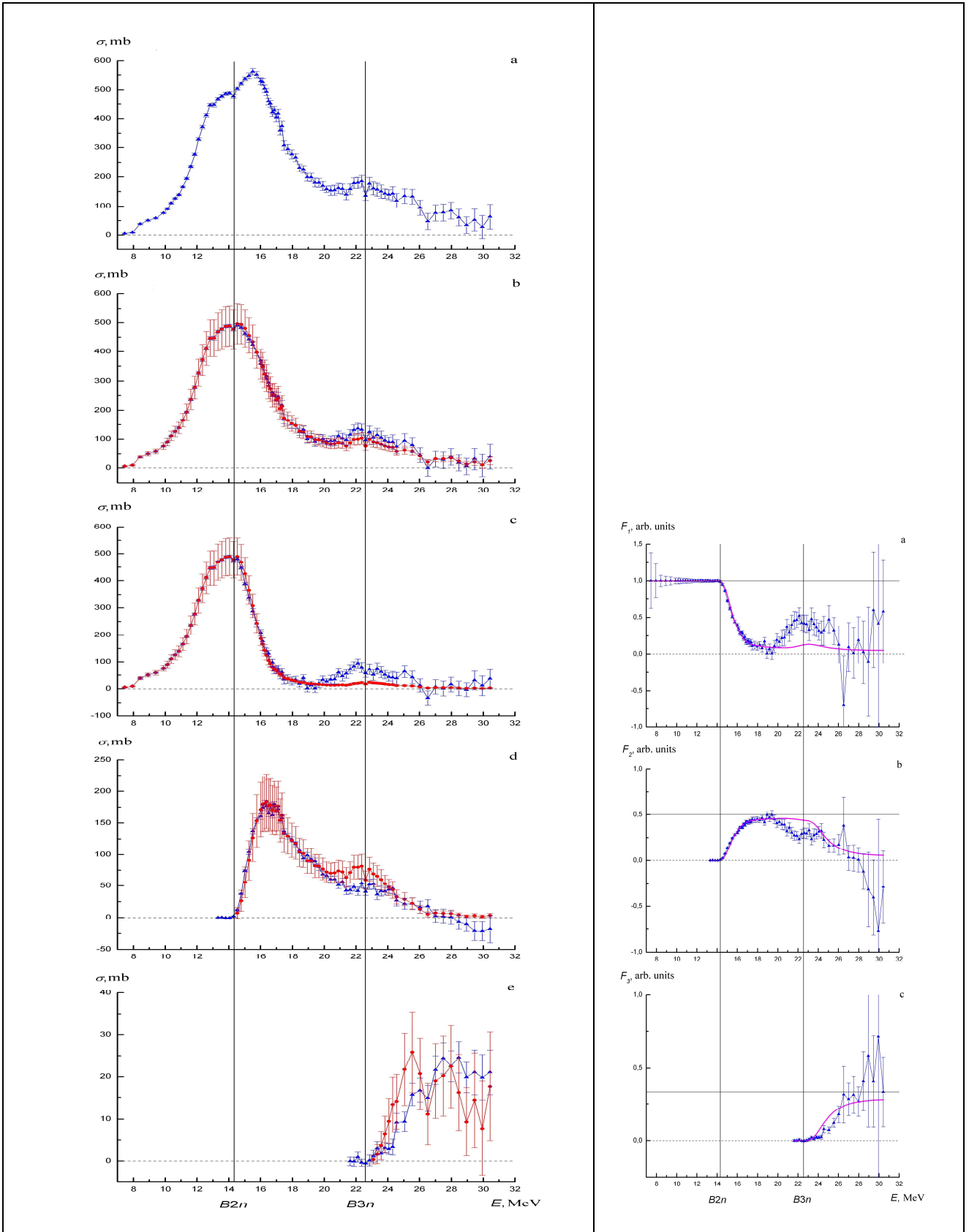


Fig. 12. Evaluated cross sections and transitional neutron multiplicity functions for  $^{188}\text{Os}$ .  
 Left: evaluated (dots) and experimental ([26] – triangles) photonuclear reaction cross sections (a –  $\sigma(\gamma, Sn)$ , b –  $\sigma(\gamma, tot)$ , c –  $\sigma(\gamma, n)$ , d –  $\sigma(\gamma, 2n)$ , e –  $\sigma(\gamma, 3n)$ ).  
 Right: experimental ([26] – triangles) and theoretical ([15, 16] – lines) multiplicity functions  $F_1$  (a),  $F_2$  (b) and  $F_3$  (c).

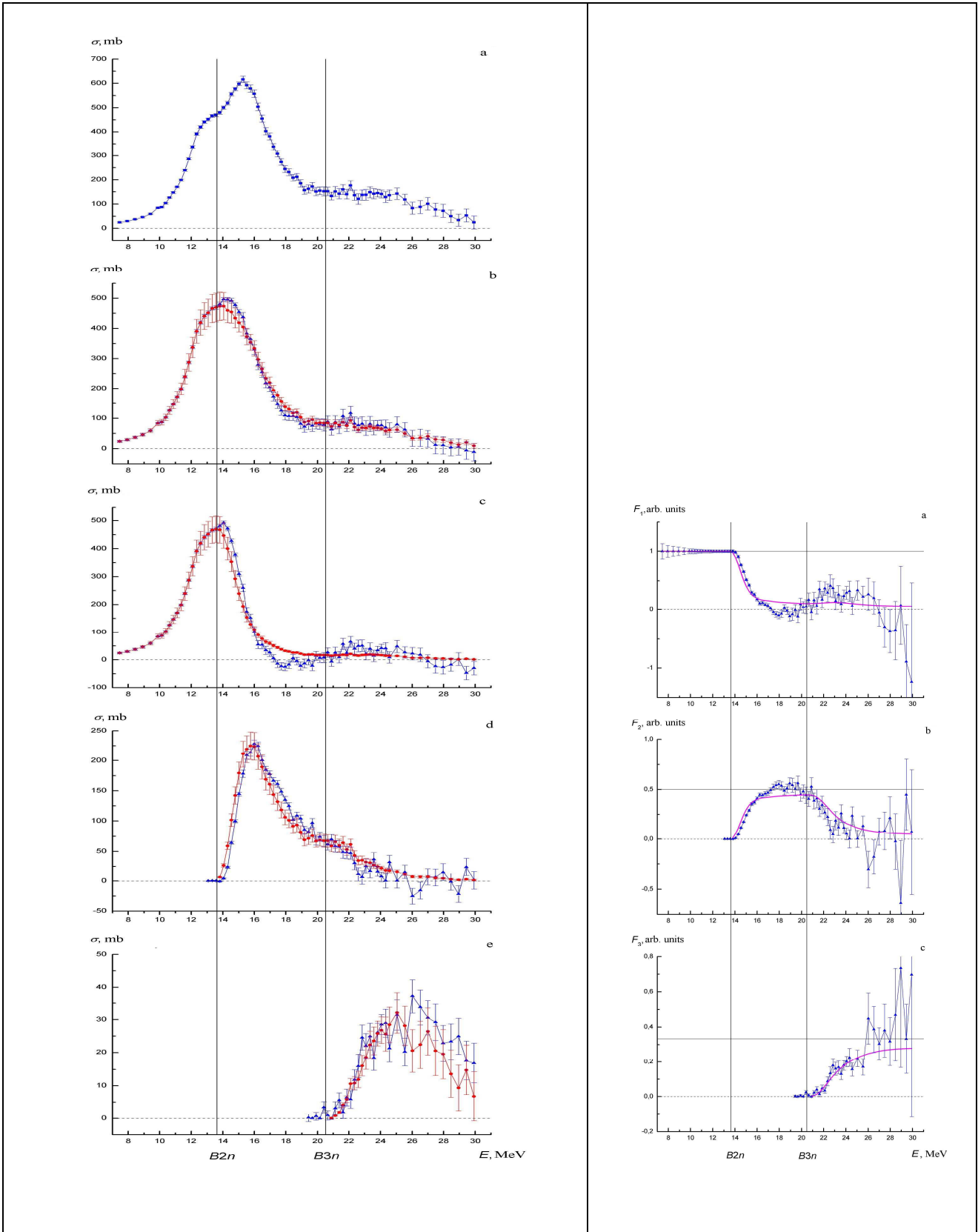


Fig. 13. Evaluated cross sections and transitional neutron multiplicity functions for  $^{189}\text{Os}$ .  
 Left: evaluated (dots) and experimental ([26] – triangles) photonuclear reaction cross sections (a –  $\sigma(\gamma, \text{Sn})$ , b –  $\sigma(\gamma, \text{tot})$ , c –  $\sigma(\gamma, \text{n})$ , d –  $\sigma(\gamma, 2\text{n})$ , e –  $\sigma(\gamma, 3\text{n})$ ).  
 Right: experimental ([26] – triangles) and theoretical ([15, 16] – lines) multiplicity functions  $F_1$  (a),  $F_2$  (b) and  $F_3$  (c).

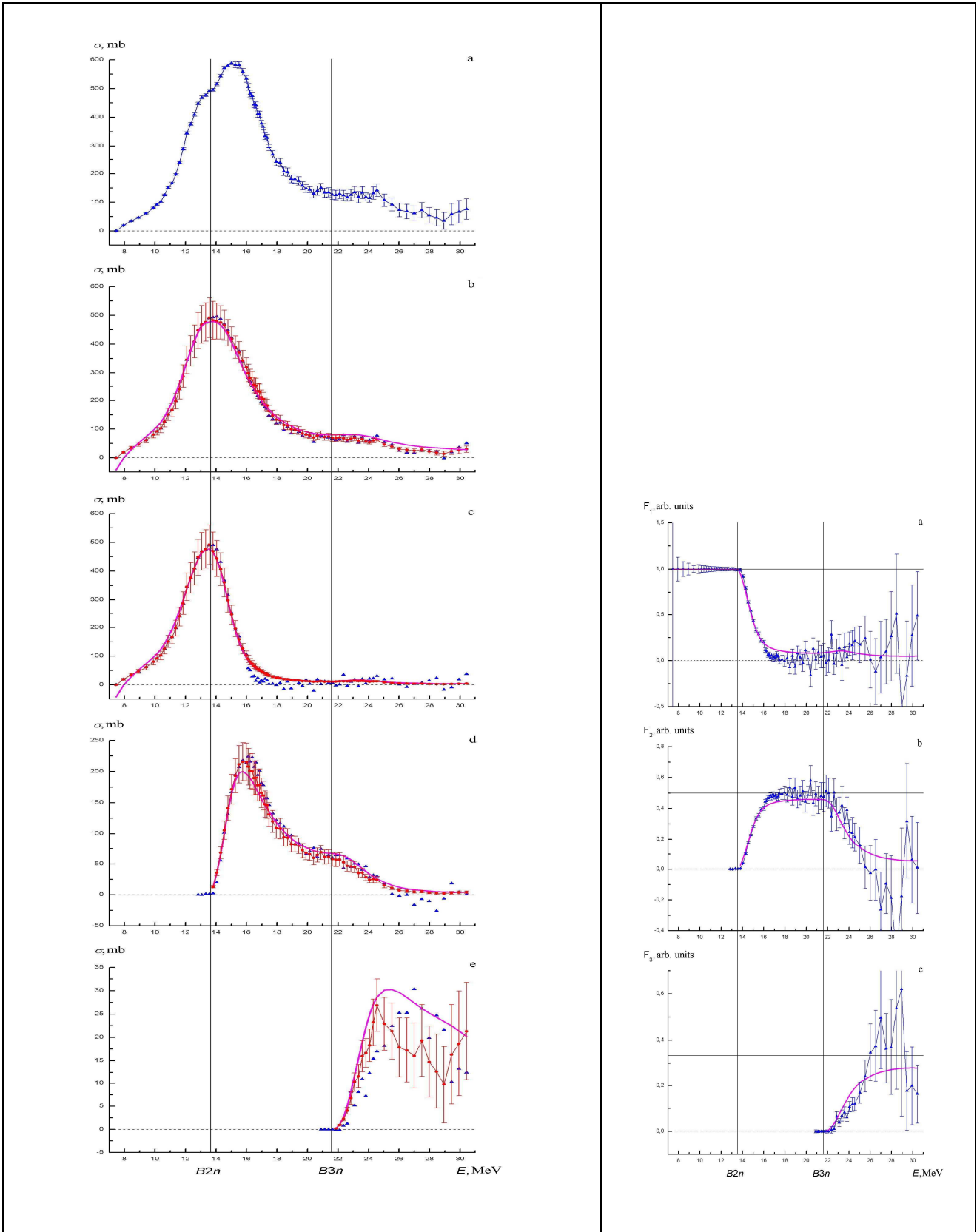


Fig. 14. Evaluated cross sections and transitional neutron multiplicity functions for  $^{190}\text{Os}$ .  
 Left: evaluated (dots) and experimental ([26] – triangles) photonuclear reaction cross sections (a –  $\sigma(\gamma, \text{Sn})$ , b –  $\sigma(\gamma, \text{tot})$ , c –  $\sigma(\gamma, n)$ , d –  $\sigma(\gamma, 2n)$ , e –  $\sigma(\gamma, 3n)$ ).  
 Right: experimental ([26] – triangles) and theoretical ([15, 16] – lines) multiplicity functions  $F_1$  (a),  $F_2$  (b) and  $F_3$  (c).

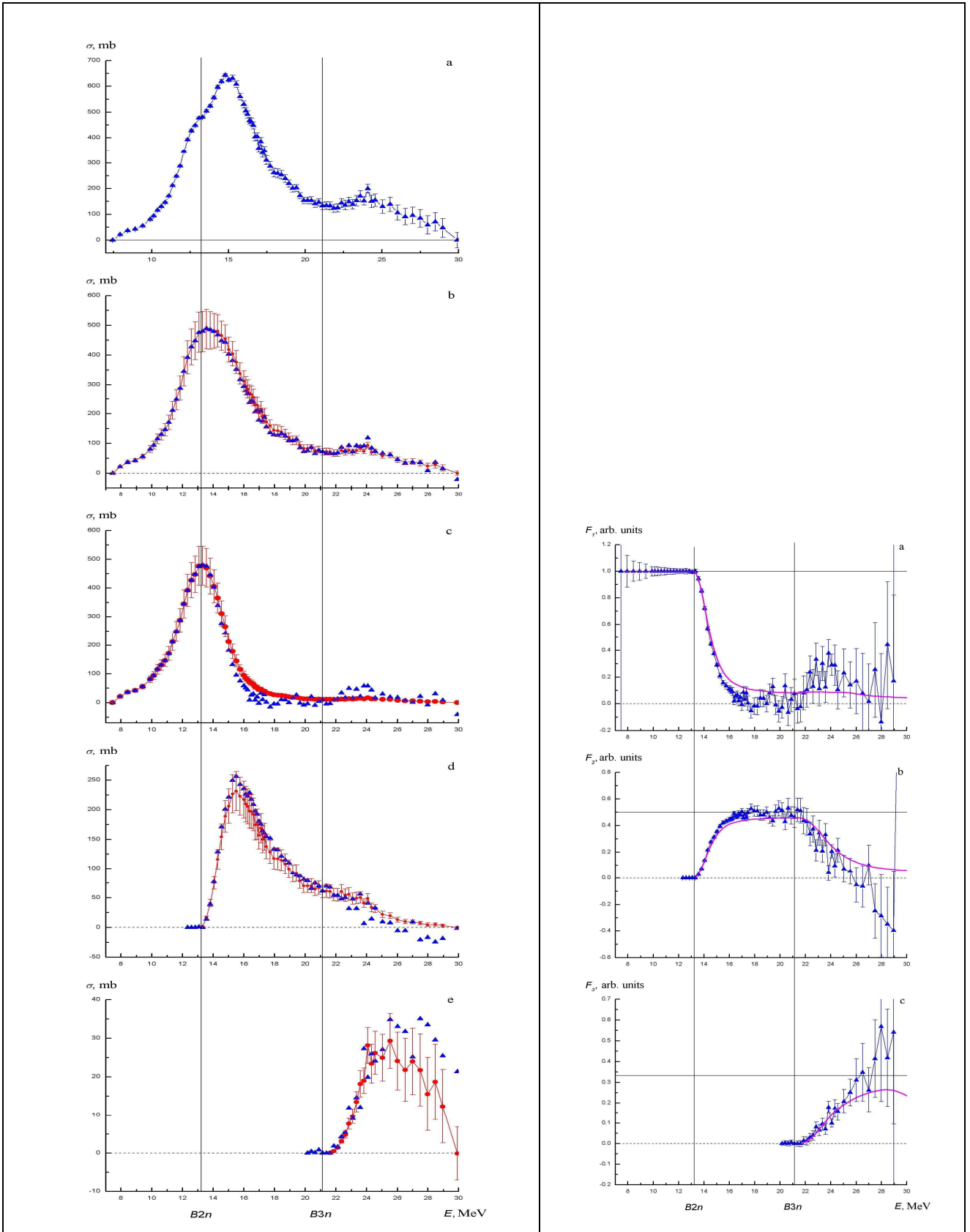


Fig. 15. Evaluated cross sections and transitional neutron multiplicity functions for  $^{192}\text{Os}$ .  
 Left: evaluated (dots) and experimental ([26] – triangles) photonuclear reaction cross sections (a –  $\sigma(\gamma, \text{Sn})$ , b –  $\sigma(\gamma, \text{tot})$ , c –  $\sigma(\gamma, n)$ , d –  $\sigma(\gamma, 2n)$ , e –  $\sigma(\gamma, 3n)$ ).  
 Right: experimental ([26] – triangles) and theoretical ([15, 16] – lines) multiplicity functions  $F_1$  (a),  $F_2$  (b) and  $F_3$  (c).

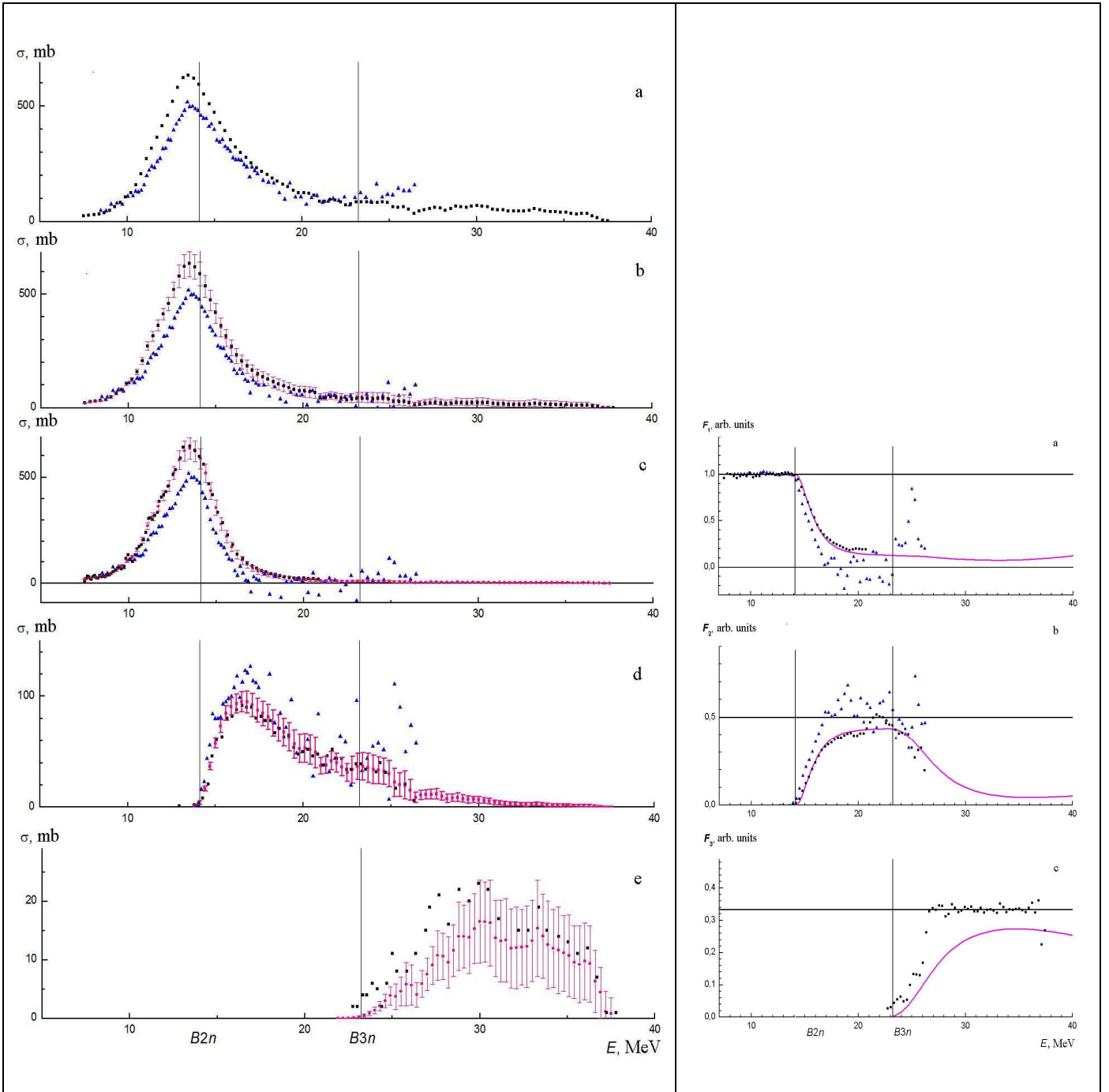


Fig. 16. Evaluated cross sections and transitional neutron multiplicity functions for  $^{208}\text{Pb}$ .  
 Left: evaluated (dots) and experimental ([27] – triangles, [33] - squares) photonuclear reaction cross sections (a –  $\sigma(\gamma, \text{Sn})$ , b –  $\sigma(\gamma, \text{tot})$ , c –  $\sigma(\gamma, \text{n})$ , d –  $\sigma(\gamma, 2\text{n})$ , e –  $\sigma(\gamma, 3\text{n})$ ).  
 Right: experimental ([27] – triangles) and theoretical ([15, 16] – lines) multiplicity functions  $F_1$  (a),  $F_2$  (b) and  $F_3$  (c).

**Борис Саркисович Ишханов  
Вадим Николаевич Орлин  
Николай Николаевич Песков  
Михаил Евгеньевич Степанов  
Владимир Васильевич Варламов**

**СИСТЕМАТИЧЕСКИЕ РАСХОЖДЕНИЯ СЕЧЕНИЙ ПАРЦИАЛЬНЫХ  
ФОТОНЕЙТРОННЫХ РЕАКЦИЙ:  
НОВЫЙ ПОДХОД К АНАЛИЗУ И ОЦЕНКЕ**

Препринт НИИЯФ МГУ 2013–1/884

Работа поступила в ОНТИ 09.09.2013